



## A Computation to Generate 2D and 3D Vector Displacements Using InSAR Ascending and Descending Source Data (Case Studies: Landslides and Earthquake in Indonesia)

NOORLAILA HAYATI<sup>1,2</sup>, WOLFGANG NIEMEIER<sup>2</sup>, PUTRA MAULIDA<sup>1</sup>, FILSA BIORESITA<sup>1</sup>, and HESTY WAHYU NURYANI<sup>1</sup>

<sup>1</sup>Department of Geomatic Engineering, Institut Teknologi Sepuluh November, Surabaya, Indonesia

<sup>2</sup>Institute of Geodesy and Photogrammetry, Technische Universität Braunschweig,  
Braunschweig, Germany

Corresponding author: [noorlaila@geodesy.its.ac.id](mailto:noorlaila@geodesy.its.ac.id)

Manuscript received: May, 6, 2020; revised: January, 15, 2022;

approved: May, 31, 2023; available online: October, 10, 2023

**Abstract** – Interferometric Synthetic Aperture Radar (InSAR) is a radar technique to generate map of surface deformation using phase differences acquired at different times. The InSAR technique measures these phase differences in its line of sight (LOS). Regarding LOS projection to a ground coordinate system, the combination of SAR data from ascending and descending can estimate at least two dimensional fields which are vertical and east-west components and three dimensional fields with either an additional motion model or vector displacements from along-track direction. The purpose of this work is to generate 2D and 3D vector displacements from two different InSAR tracks (e.g. ascending and descending) with a calculation programme both for the mean velocity and time series data named as PS DISP. 2D mode is calculated in which the north-south component is neglected due to insensitive along the flight direction, thus, assuming to be zero (0). On the other hand, 3D mode is calculated with an assumption that the north-south component moves along the elevation downward. The experimental results were conducted for the Puncak Pass and Puncak Highway landslides and the Lombok earthquake in Indonesia. For the landslide study, the computation generated the movement towards the slope surface in the 3D Cartesian coordinate ( $d_U$ ,  $d_E$  and  $d_N$  (psuedo)) and found both the crown body and cumulative zone of the landslide. For the earthquake study, PS DISP decomposed 2D vectors ( $d_V$  and  $d_E$ ). The area of earthquake rupture was lifted by 42 cm and other northern Lombok areas by 10 - 25 cm. Regarding the west-eastern motion, it shows that the west of northern Lombok was displaced  $\pm 5$  cm toward the west direction, while the other side to the east direction.

**Keywords:** InSAR, 2D and 3D displacements, slope aspect, ground motion, landslide, earthquake

© IJOG - 2023

### How to cite this article:

Hayati, N., Niemeier, W., Maulida, P., Bioresita, F., and Nuryani, H.W., 2023. A Computation to Generate 2D and 3D Vector Displacements Using InSAR Ascending and Descending Source Data (Case Studies: Landslides and Earthquake in Indonesia). *Indonesian Journal on Geoscience*, 10 (3), p.323-334. DOI: [10.17014/ijog.10.3.323-334](https://doi.org/10.17014/ijog.10.3.323-334)

## INTRODUCTION

### Background

One of the limited InSAR applications to observe ground surface movement is the geometrical motion seen along the line of sight. In

practice, it needs to project the LOS displacement to 3D (vertical, east-west, and north-south direction) vectors. They are easier to identify the ground movement characteristics than along the satellite range view. Several researchers have developed variety methods to solve this problem.

It can be solved by a combination from other geodetic measurements, such as GPS (Global Positioning System) (Vollrath *et al.*, 2017) and Ground-based Radar (Provost, 2018), retrieving from slant range and along-track direction using two different orbits (Bechor and Zebker, 2006; Hu *et al.*, 2014; Grandin *et al.*, 2016) for swath mode, and different incidence angle from left-right looking (Wright *et al.*, 2004).

Although not all of geo-environment case studies could be retrieved by the full displacement vectors, 2D vectors (vertical and east-west components) are commonly computed from the source of ascending and descending SAR data with neglecting the north-south vector. Another option is using an assumption at the characteristics of displacement. For example, glacier flow monitoring has a tendency moving parallel to surface gradient (Mohr, 1997). It takes into account for Persistent Scatterer DISplacement (PS DISP) to decompose the full displacement by adding the aspect information in 3D mode computation.

This paper explains the work of PS DISP script. It is a bundle script written in bash shell and Matlab code. The script requires Generic Mapping Tools (GMT) and Matlab Software and runs under the Linux operating system. The output for 2D mode is the vertical ( $d_V$ ) and east-westward ( $d_E$ ) vectors. 2D mode is appropriate to study cases such as subsidence, crustal deformation, and any other deformation phenomena in which the direction of movement can not be predicted easily. Meanwhile, the output for 3D mode is the vertical ( $d_V$ ), east-westward ( $d_E$ ) and north-southward ( $d_N$ ) vectors. 3D mode is computed based on the elevation downward behaviour. It is assumed that the movement will be going to the lower level due to the gravitational effect. It is a pseudo calculation for the third component of 3D vectors using the aspect information. 3D mode could be used to study cases such as landslide (slow movement), glacier monitoring, volcano observation, *etc.* In addition, 3D combo could be used to retrieve the full components in condition for an extremely high deformation, for example devastated earthquake

before and after the main shock. It requires SAR data computed both slant-range or across-track direction (conventional InSAR method) and along-track direction *e.g.* azimuth, amplitude, pixel offset or multiple aperture InSAR (MAI) methods processing data.

To be considered by end-user using this script, the background of three modes on PS DISP can be described as follows:

The output vectors from 2D mode have an assumption to neglect south-north motion. Originally, the sensitivity decomposition of horizontal displacement on the pole direction still remains -0.07 for  $d_N$  compared to 0.92 for  $d_V$  and 0.38 for  $d_E$  in terms of  $\theta_{inc} \approx 23^\circ$  and  $\alpha_h \approx 190^\circ$  (Hanssen, 2001).

3D mode takes account of  $d_N$  component as a pseudo output. It is only a transform projection in scheme of horizontal displacement using the estimation of down-slope direction from each cell to its neighbours. This method is only appropriate to the case study having a motion parallel to the surface, for instance slowly slope movement and glacier flow.

3D combo is the most appropriate method to retrieve full displacement vectors. However, not all of case studies could be observed both across track and along track interferometry, namely different viewing geometry. Hence, it is only suitable for a high deformation phenomenon, such as earthquake.

The computation was applied to two real studied areas to examine the feasibility of these methods. Ciloto Subagency is the studied area with a slowly moving landslide used to assess 3D mode, since it moves towards downhill and surface deformation. Lombok earthquake was used to perform 2D mode, since its movement can be identified based on surface fractures. The result of 2D mode will be validated with the deformation model computed by Okada model (Okada, 1985; 1992). Both studied areas are located in Indonesia. However, 3D combo was not inspected in this research, because the limited SAR data and improper case studies to generate the techniques of along the track direction decomposing 3D vectors.

## METHODS AND MATERIALS

### Methods

According to Hanssen (2001) the LOS projection ( $d_{LOS}$ ) to  $d_U$  for vertical,  $d_E$  for west-east, and  $d_N$  for north-south components is described as:

$$d_{LOS} = d_U \cos \theta_{inc} - \sin \theta_{inc} [d_N \cos \alpha_h + d_E \sin \alpha_h] \dots\dots(1)$$

where:

$\theta_{inc}$  is the incidence angle, and

$\alpha_h$  is the satellite platform heading angle  $-3\pi/2$  either on ascending ( $_{asc}$ ) or descending ( $_{dsc}$ ) orbit.

PS DISP uses the ordinary least square (OLS) solution to the linear system of the following equations. Several modes that could be chosen to derive the vectors are as follows:

#### 2D Mode

On 2D mode, it decomposes only two components which are vertical and west-east assuming the north-south is zero (0). This is a common applied method if the data are present both along ascending and descending orbits.

$$\begin{bmatrix} \cos \theta_{incasc} & -\sin \theta_{incasc} \cdot \sin \alpha_{hasc} \\ \cos \theta_{incdsc} & -\sin \theta_{incdsc} \cdot \sin \alpha_{hdsc} \end{bmatrix} \cdot \begin{bmatrix} d_U \\ d_E \end{bmatrix} = \begin{bmatrix} d_{losasc} \\ d_{losdsc} \end{bmatrix} \dots(2)$$

#### 3D Mode

On 3D mode, PS DISP takes into account the assumption of movement parallel to the surface elevation. Therefore, aspect angle  $\theta_{asp}$  was derived from external elevation model, for example SRTM3 or TanDEM X is needed for projecting  $d_E$  to  $d_N$ . The detailed description of this assumption can be read on Isya *et al.* (2019) as below:

$$\begin{bmatrix} \cos \theta_{incasc} & -\sin \theta_{incasc} \cdot \sin \alpha_{hasc} & -\sin \theta_{incasc} \cdot \cos \alpha_{hasc} \\ \cos \theta_{incdsc} & -\sin \theta_{incdsc} \cdot \sin \alpha_{hdsc} & -\sin \theta_{incdsc} \cdot \cos \alpha_{hdsc} \\ 0 & \cos \theta_{asp} \cdot \cos(90 - \theta_{asp}) & -1 \end{bmatrix} \cdot \begin{bmatrix} d_U \\ d_E \\ d_N \end{bmatrix} = \begin{bmatrix} d_{losasc} \\ d_{losdsc} \\ 0 \end{bmatrix} \dots(3)$$

#### 3D Combo

On 3D combo, the decomposition of full vector displacement is calculated both from across-track (slant-range) and along-track directions. This is the best scenario to retrieve them. However, the application limits only for the case study having high correlated area and an extreme deformation which might be detected using azi-

muth offset, MAI, or burst overlap interferometry method (Equation 4).

$$\begin{bmatrix} \cos \theta_{incasc} & -\sin \theta_{incasc} \cdot \sin \alpha_{hasc} & -\sin \theta_{incasc} \cdot \cos \alpha_{hasc} \\ \cos \theta_{incdsc} & -\sin \theta_{incdsc} \cdot \sin \alpha_{hdsc} & -\sin \theta_{incdsc} \cdot \cos \alpha_{hdsc} \\ 0 & \sin \alpha_{hasc} & \cos \alpha_{hasc} \\ 0 & \sin \alpha_{hdsc} & \cos \alpha_{hdsc} \end{bmatrix} \cdot \begin{bmatrix} d_U \\ d_E \\ d_N \end{bmatrix} = \begin{bmatrix} d_{losasc} \\ d_{losdsc} \\ d_{aziasc} \\ d_{azidsc} \end{bmatrix} \dots(4)$$

#### Three criteria for assessing the solutions are:

- The SAR data from ascending and descending spatially must be overlaid on the same region (set on PS DISP parameter file as "region").
- As a combined result of different orbit, the near neighbour method must match the PS scatters from those orbit data in certain radius, and later it resamples to certain resolution given by user ("radius" and "resolution").
- The gridding surface method must have greater PS numbers than the near neighbour, because the grid table function must fully fill the NaN pixels as a result of adjustable interpolation from its neighbour. To avoid the overestimated PS pixels on unwanted areas, PS DISP controls the final matching procedure using a parameter from amplitude dispersion index.
- The input data could be imported from GMT-SAR (Sandwell *et al.*, 2016) and StaMPS (Hooper *et al.*, 2012) processing or external data (limited to only nearest neighbour method).

The script computes the SAR data both from the mean velocity and time series results. The first step is that PS DISP will find the matching ascending and descending data using surface or near neighbour method. The surface method is a function on GMT software which makes gridding based on adjustable tension continuous curvature splines (Smith *et al.*, 1990). In avoiding the extrapolation at uncorrelated area, the grid table was controlled by amplitude dispersion parameter for single master (SM) and amplitude difference dispersion for small baseline (SB) networks. On the other hand, the near neighbour method does not require amplitude dispersion. Instead, it only matches the scatters (pixels) between those resampling pair results. The near neighbour is also a function from GMT in purpose to grid the table data using "the near-

est neighbour" algorithm. There is a section to resample in spatial and interpolate in time for time series data.

A further step, it generates  $d_U$ ,  $d_E$  and  $d_N$  vector displacements using OLS function in Matlab software. To help user interpreting the results, PS DISP has a mode to plot the vertical displacement using surface model and horizontal displacement using vector velocity. In addition, simple statistics could be run as well. A brief process chain of PS DISP could be seen in Figure 1.

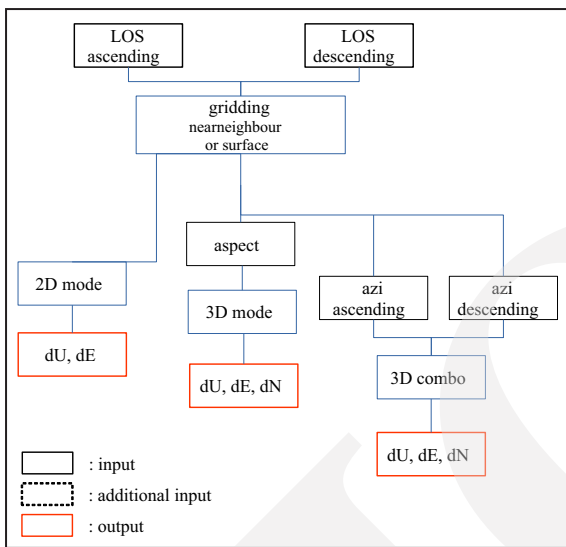


Figure 1. PS DISP process chain.

**Materials**

Sentinel-1 SAR data from 2014 to 2018 were used to monitor the time series displacement in Ciloto. All images were taken from ascending and descending source data with interval time either twelve or twenty-four days. Furthermore, four pairs of Sentinel-1 images on 27<sup>th</sup> July 2018 - 8<sup>th</sup> August 2018, 2<sup>nd</sup> August 2018 - 8<sup>th</sup> August 2020, 30<sup>th</sup> July 2018 - 5<sup>th</sup> August 2018, and 30<sup>th</sup> July 2018 - 11<sup>th</sup> August 2018 were used to detect the surface movement due to the Lombok earthquake in 2018 for the two pairs of ascending and descending orbit, respectively. Table 1 shows data and their details used in this research. Two different InSAR method were utilized in order to produce LOS displacement. It is based on different phenomena which are Small Baseline with Slowly Decorrelating Filter Phase (SDFP) (Hooper, 2008) for slow rate movement monitoring in the risk landslide area of Ciloto and two-pass Differential InSAR (DInSAR) (Ding and Huang, 2011) for deformation measurement in the event of Lombok earthquake. SRTM 1 arc second was used as a digital elevation model (DEM) to reduce the effect of topography on interferograms. In addition,  $d_N$  (pseudo) of 3D Mode was generated by the slope aspect from this DEM as well.

Table 1. Material Description Used to Test PS DISP. Using the Case Study of Landslides and Earthquake in Indonesia

No	Data	Acquisition Date	Number of SAR images	Number of interferograms	Method of InSAR	Purpose	Expected Vector decomposition	Accuracy Measurement
1	Sentinel-1 A/B, the ascending track with the path of 98, the descending track with the path of 47	From October 2014 until June 2018	Ascending = 72 images, Descending = 68 images	Ascending = 341, Descending = 349	Small Baseline with slowly Decorrelating Filter Phase (SDFP)	Slow movement monitoring in the potential landslide area	Time series of $d_U$ , $d_E$ , $d_N$ (pseudo)	mm - unit
2	Sentinel-1 A, the ascending track with the path of 156, the descending track with the path of 32	Ascending = July 30 & August 02, 2018 as master and August 08, 2018 as slave Descending = July 30, 2018 as master and August 05 & 11, 2018 as slave	Ascending = 3 images Descending = 3 images	Ascending = 2, Descending = 2	two-pass DInSAR	Deformation detection due to earthquake effect	Displacement of $d_U$ , $d_E$	cm - unit

## RESULT AND ANALYSIS

### PS DISP has been tested to areas as follows:

- **Ciloto:** One of the most prone landslide areas in Indonesia where significantly slow creep movement are recorded in recent years (Arifianti *et al.*, 2020). Sentinel-1A/B data have been processed from 2014 to the middle of 2018. A 3D mode was used to generate full vector displacement which  $d_N$  takes into account as a pseudo component. The assumption is that deformation moves towards downhill. Considering the natural characteristics of a landslide, its direction will be parallel to the aspect of downslope surface. The detail can be read from a previous research (Isya *et al.*, 2019).
- **Lombok:** The north region of Nusa Tenggara Barat Province was suffered from 7.0 magnitude of the main shock earthquake on August 5<sup>th</sup> 2018. This second study performed data processing to obtain the deformation values of the slave and master direction ascending and descending after the Lombok 5<sup>th</sup> August 2018 earthquake using Sentinel-1A SLC imagery with the DInSAR two-pass interferometry. The results are 2D displacements in the west-east direction (X axis) and vertical direction (Z axis). The 2D mode was used to decompose 2D vectors ( $d_U$  and  $d_E$ ) and assuming that  $d_N$  is zero since SAR orbits are insensitive towards polar direction.

### Ciloto Landslide

The first test has been done on a slow movement case study. 3D mode based on aspect information confirmed a detection of slope movement in Puncak Pass and Puncak Highway regions. Figure 2 shows the cumulative displacement both vertical and horizontal directions in Puncak Pass where a landslide occurred on March 28<sup>th</sup> 2018. Although the area is covered by vegetation indicating noisy signal, there are still some man-made objects such as street, poles, and buildings detected as PSs.

Eighteen PS samples have been assessed at the top region (106.993892° – 106.994032°; -6.706263° – -6.705995°) classified as the crown

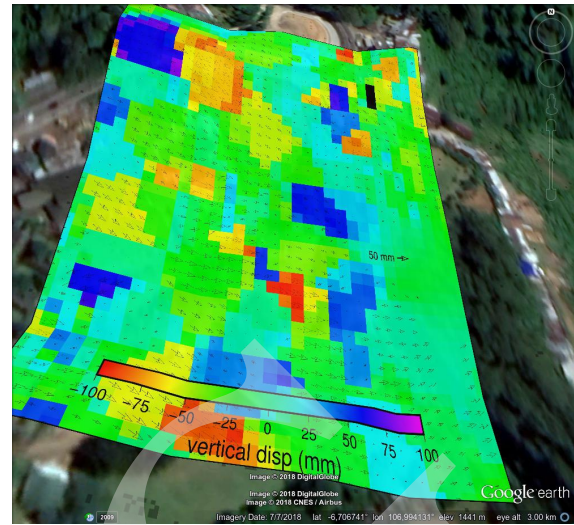


Figure 2. Cumulative displacement until December 2018 in Puncak Pass, Ciloto. The vertical motion is shown by colour and the horizontal with the 0.005 scale arrow symbol. The top and bottom black boxes are the location of a landslide crown and a deposit area, respectively.

landslide body and twenty-two PSs at the bottom area (106.994131° – 106.994317°; -6.706589° – -6.706368°) indicated as a cumulative zone of landslide. Since a landslide occurred in the range of processing dates, the phase jump more than  $\pm\pi/2$  cannot be easily corrected (Notti *et al.*, 2015) as one unwrapping error. Hence, this drawback might be an indication of the break point for the slope failure viewed by SAR multitemporal data as shown in Figure 3.

Another observed location is Puncak Highway. Several geodetic measurements (the terrestrial and GPS monitoring) had been conducted from 1995 until 2013 (Sadarviana, 2006). With the available SAR space-borne sensors, the region has a high possibility to be continuously and efficiently monitored with the aim of supporting the early warning system for a landslide hazard. Figure 4 shows that the generated 3D vectors indicating the hill is still moving  $-17\pm 6$ ,  $4\pm 3$ ,  $-1\pm 0.7$  mm/year for  $d_U$ ,  $d_E$ ,  $d_N$  respectively are assumed as a linear deformation. For time series computation, sixty-nine PS samples located near Puncak Highway and local houses (107.005747° – 107.006218°; -6.714181° – -6.713686°) were plotted for each component as shown in Figure 5. The cumulative displacements until the last date

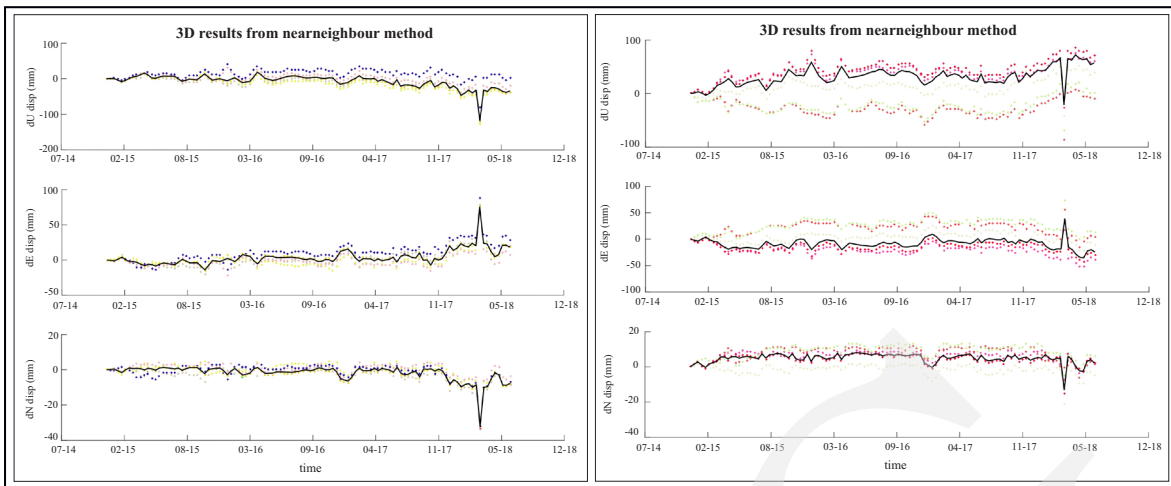


Figure 3. Time series plot for 3D vectors displacement. The left graphic indicates a down-lift zone towards southeastern direction and the right indicates a cumulative zone with a small horizontal motion towards northwest. The strip line is a break time point of landslide collapse in that area.

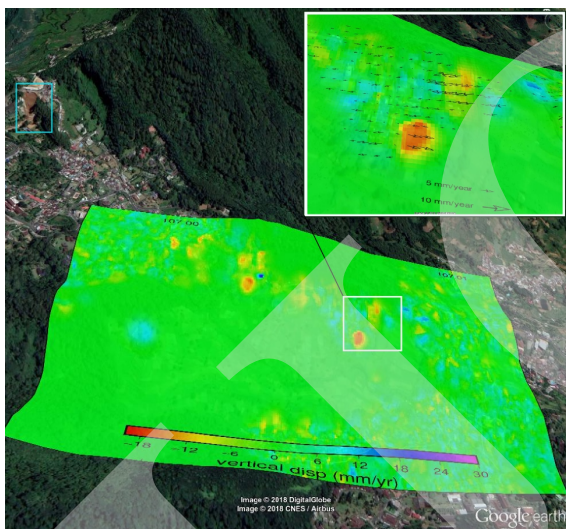


Figure 4. Mean velocity around Puncak Highway area. White box shows significant down-lift motions near the highway and local houses. A colour scale represents vertical displacement and an arrow implements horizontal displacement. Meanwhile, a cyan box is location of Puncak Pass described in Figure 3.

of processing from December 11<sup>th</sup> 2014 to June 17<sup>th</sup> 2018 describe that the region of interest had moving to  $-63 \pm 25$ ,  $24 \pm 11$ ,  $-5 \pm 2$  mm for  $d_U$ ,  $d_E$ ,  $d_N$  in average, respectively. As an analysis of these vectors, it is characterized that the slope is slowly sinking towards southeast direction. However, there is no indication of up-lift or deposit zone near the region since the region has limited PS numbers because of agricultural land use and

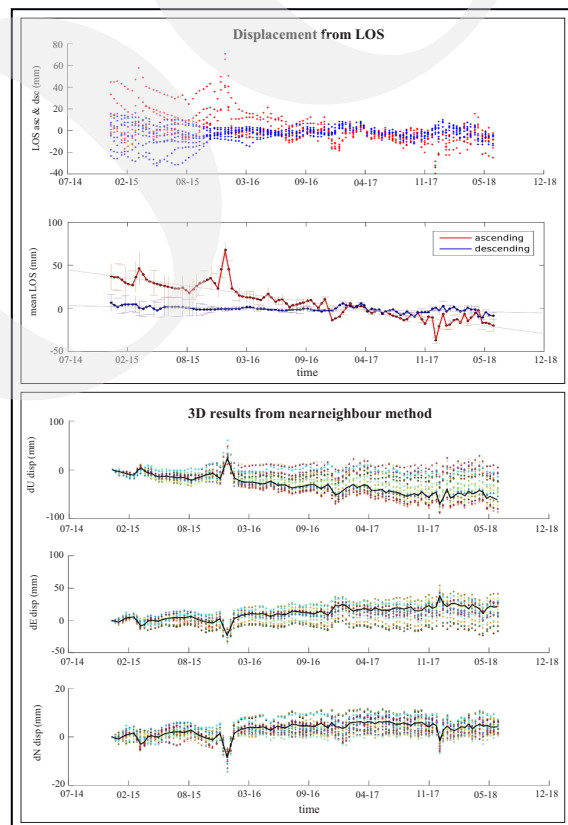


Figure 5. Sixty-five PSs collected near Puncak Highway and local houses. Top picture describes LOS displacement with error bar (standard deviation) both ascending and descending, while the bottom one describes 3D vector outcome. The generated 3D result shows down-lift motion for vertical and moving towards southeast for horizontal component. Because of the slope faces the west, ascending SAR data are more suitable to detect surface change along the line of sight.

consequently decreasing due to a match result between ascending and descending data.

Considering  $d_N$  vector as a "pseudo" 3D outcome, the quality of this projection is depending on DEM accuracy to the real terrain. On the test, Ciloto aspect information is generated from SRTMv3 about 30 m resolution which might not be representative of the precisely local terrain along the slope. Another point of view, landslide is a complex slope instability phenomenon which the characteristics of movement is not only influenced by gravitational force towards down-slope but also the physical parameters, for instance lithology, geological structures, ground water flow, and drainage lines.

### Lombok Earthquake

The main shock of 7 magnitude hit Nusa Tenggara Barat on August 5<sup>th</sup> 2018. It has been reported that 563 people died and thousands loss their houses after the main shock event. The Indonesian BMKG (Indonesian Agency for Meteorology, Climatology, and Geophysics) announced that the Lombok earthquake is a group of five thrust type earthquakes with the epicentre is located near the north of Rinjani Volcano (Ramdani *et al.*, 2019), which are:

- A foreshock 6.4  $M_L$  on July 29<sup>th</sup> 2018 at a shallow depth of 14 km (the white star symbol in Figure 6);
- The mainshock 7.0  $M_L$  on August 5<sup>th</sup> 2018 at a depth of 15 km (the red star symbol in Figure 6);
- An aftershock 5.9  $M_L$  on August 9<sup>th</sup> 2018;
- An aftershock 6.4  $M_L$  on August 18<sup>th</sup> 2018;
- A new major earthquake from a different fault 5.9  $M_L$  on August 19<sup>th</sup> 2018 at a depth of 25.6 km (the yellow star symbol in Figure 6).

The trigger of the main shock event is clearly due to the foreshock occurred a week before with the length between two epicentres is about 10 km. The tectonic earthquake swarm is caused by a shallow thrust fault near Flores Back-Arc Thrust. PUSGEN (National Centre for Earthquake Studies) described that the fault at north of Lombok was divided into two segments. One segment has

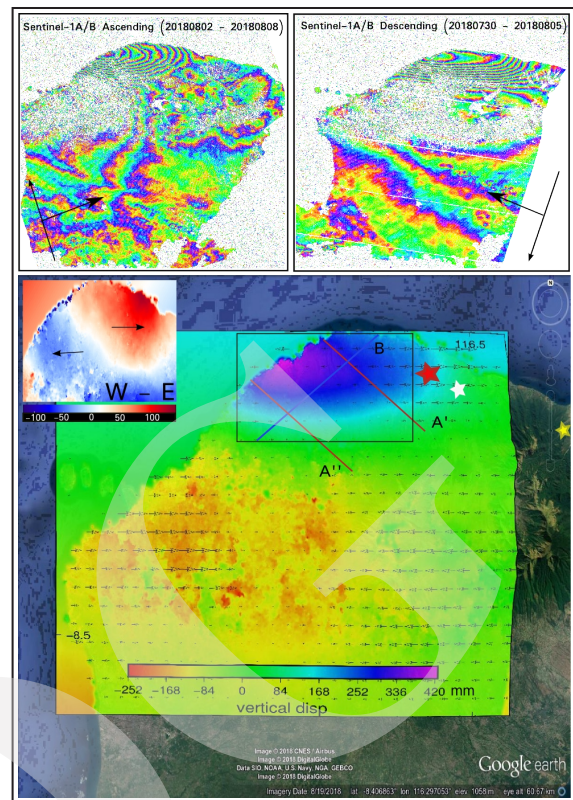


Figure 6. Vertical and west-east displacement result after the main shock earthquake in Lombok.

a potential force until 7.5  $M_L$ . Regarding InSAR 2D displacement result, the area of earthquake rupture has been lifted by 42 cm, and the other northern Lombok areas by 10 - 25 cm. Meanwhile, the southern rupture indicates down-lift movement until -25 cm including Mount Rinjani decreasing about -16 cm on its height. However, the southern part is suffered by decorrelated signals, and makes its pixel value only based on a gridded result of continuous curvature splines. It involves the extrapolation in poorly constrained region. Moreover, a further research should be conducted to provide a detail, whether the phase change contributes as an atmospheric artifact, unknown noise, or indeed a real crustal deformation.

Regarding the west-east motion, it shows that the west of northern Lombok is displaced  $\pm 5$  cm toward the west direction, while the other side to the east direction (Figure 7a). Meanwhile, the southern part (placed at low coherence area) behaves on the contrary to northern part that both sides move toward to the middle zone (Figure 7b)

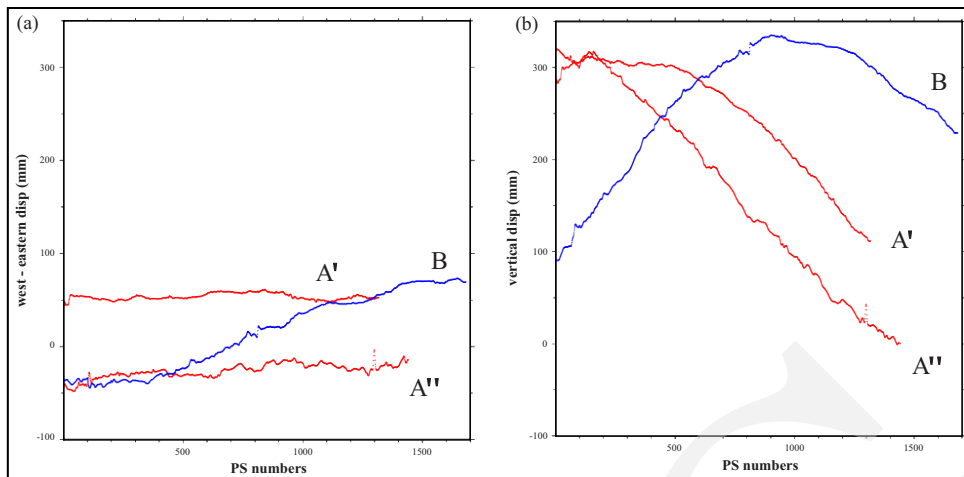


Figure 7. Displacements based on profile lines in Figure 6; a) Horizontal west-east and b) Vertical

between Pemenang District and Mount Rinjani. Since the deformation map was generated by the InSAR technique only from the slant range direction (across track) in purpose to detect the surface movement induced by the Lombok earthquake, it is better for a future work to consider SAR processing both across-track and along-track views. Therefore, the complete three vector displacements could be generated using 3D Combo computation method. In addition, a validation to geophisic ground survey is necessary to define precisely the position of fault line and its segment.

**Validation with Okada Model**

Okada modeling processing requires several parameters, such as depth, strike, dip, length, width, rake, and slip as shown in Table 2. The longitude and latitude values used in the processing of the Okada model are the longitude and latitude results from the LOS to 2D decomposition. Figure 8a is the result of vertical displacement

in Okada modeling which has a value range of -0.104 to 0.376 m, and Figure 8b is the result of west–east displacement in Okada modeling which has a value range of -0.042 to 0.031 m generated by SAR Images acquisition time from July 30<sup>th</sup> 2018 to August 11<sup>th</sup> 2018. The RMSE value for the vertical direction is 0.1337 m, and the displacement for the west–east direction is 0.03 m. While the correlation coefficient value for vertical displacement is 0.933 or has a very strong correlation coefficient, and for west–east displacement has a value of 0.438.

Figure 9a shows the direction vector resulting from the displacement decomposition process, and Figure 9b is the result of Okada modeling with a grid of 5km x 5km. The direction vector is obtained from the displacement value with the vertical direction (z-axis). The arrows with blue colour indicate uplift, while the red ones indicate subsidence. It has a similar pattern but tends to have slightly different values between InSAR results and Okada modeling. This can be caused by differences in parameters definition that are distinctively used in Okada modeling processing. Figure 9c shows the vector direction of west component (red colour) and east component (blue colour) from InSAR decomposition, while the west–east vector from Okada modeling is in Figure 9d.

A graph of the deformation value between the decomposition results and Okada validation,

Table 2. Parameters of the Lombok Earthquake August 5<sup>th</sup> 2018 (Salman *et al.*, 2020)

	05/08/2018 (Mw = 6,9)
Depth	12±3 km
Strike	80°
Dip	21°
Length	38904.5145 m
Width	19849.75277 m
Rake	90°
Slip	1.230619077 m

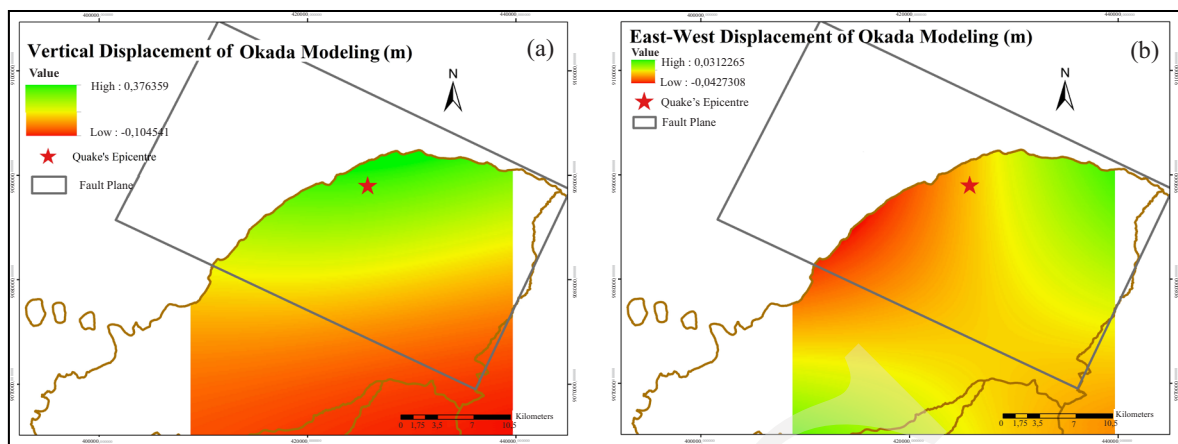


Figure 8. Result of Okada modeling displacement: a) Vertical displacement; b) West-East displacement.

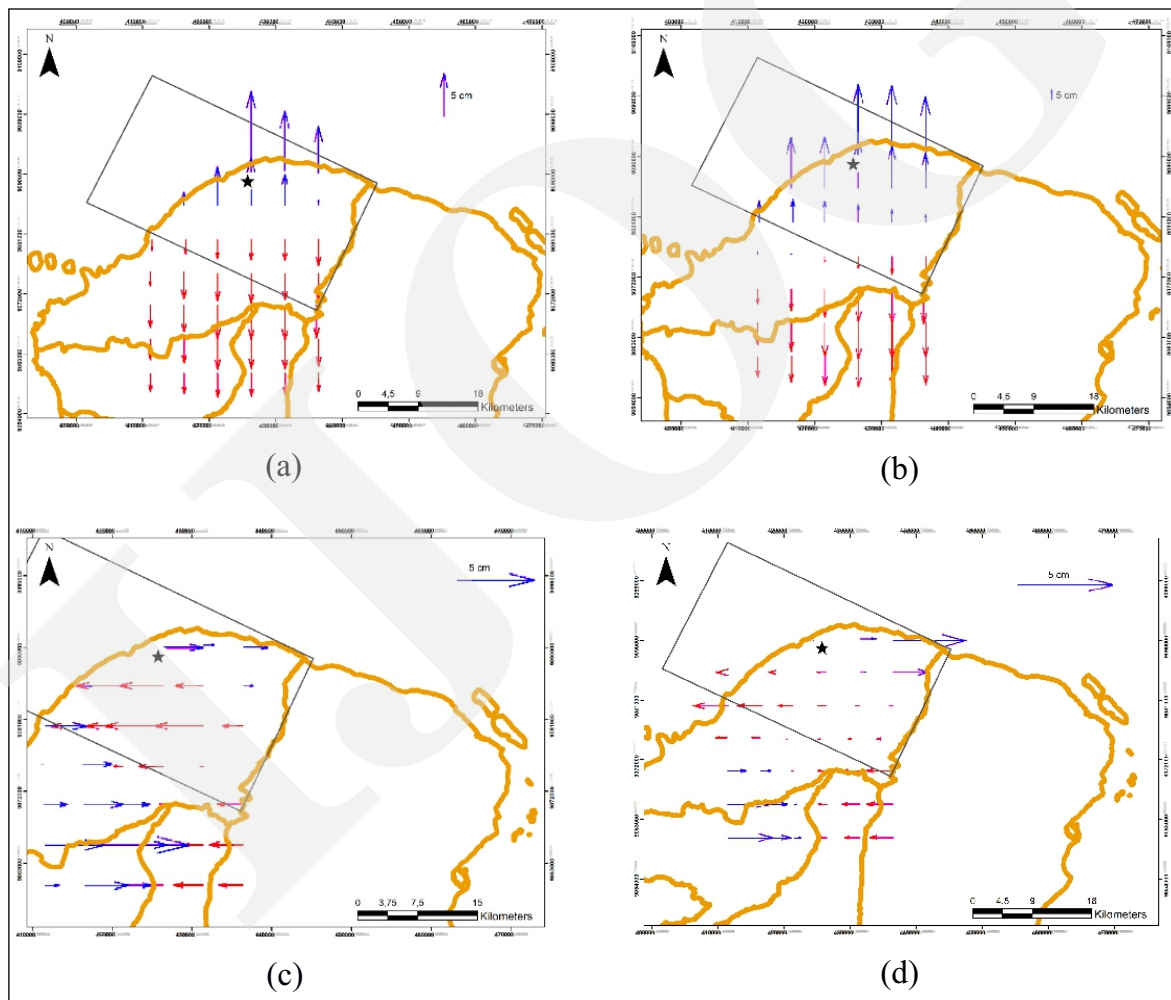


Figure 9. Vertical displacement: (a) Generated by InSAR decomposition and b) Of Okada modeling; East-West displacement: (c) Geothermal by InSAR decomposition and d) of Okada Modeling.

both in the vertical and west-east directions are shown in Figure 10. From the sample profiles, it can be seen that the deformation value of Okada

validation has a greater value than the deformation value of the decomposition results. However, the results of correlation coefficient show that

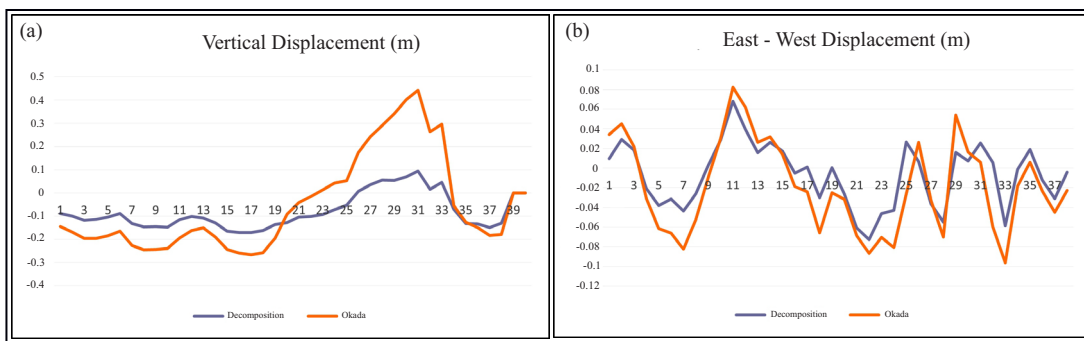


Figure 10. Sample profiles of InSAR decomposition and Okada validation both for (a) Vertical direction and (b) West-East direction.

the value of the decomposition deformation with Okada validation has a strong correlation.

The difference in the vertical and west-east displacements between the processing of DInSAR results and Okada modeling has a relatively large value, especially for the vertical displacement. This is due to differences in the definition of parameters used in the Okada modeling processing. In addition, there are other earthquakes in the SAR image recording time interval which was used for the processing. In this study, the recording time interval of twelve days was used between the master and slave images. The descending image uses a master image with a recording time of July 30<sup>th</sup> 2018 for a slave image on August 11<sup>th</sup> 2018, while on August 9<sup>th</sup> there was an aftershock earthquake in Lombok with a magnitude of 6.2. Although this aftershock earthquake has a smaller strength than the mainshock earthquake of August 5<sup>th</sup> 2018, it can still affect the results of the DInSAR processing with the results from Okada modeling. Therefore, it is supposed to do this Okada modeling using parameters from the Lombok August 5<sup>th</sup> 2018 and August 9<sup>th</sup> 2018 earthquakes, but in this study, it is only limited to the Lombok August 5<sup>th</sup> 2018 earthquake.

### CONCLUSIONS

The slow movement in Ciloto landslide areas was assessed based on the result of time series InSAR and decomposed 3D vectors based on PS DISP computation. The rate of displacement in Ciloto was in the range of -13 to 30 mm/year for

the vertical movement and the range of 5 – 10 mm/year for the horizontal one. Furthermore, the analysis of deformation after the August 5<sup>th</sup> 2018 Lombok earthquake used Sentinel-1A images with the DInSAR two-pass interferometry method. It can be concluded that based on the results of the data processing using the DInSAR two-pass interferometry method for observation of deformation on August 5<sup>th</sup> 2018 earthquake, Lombok experienced a vertical displacement range of -0.1 to 0.42 m, especially the northern Lombok region. While the west–east direction has a value range of -0.1 to 0.1 m.

For 3D mode, both the zone of depletion and accumulation was succeeded to be identified with its movement direction in Ciloto areas from 2015 to 2018. Meanwhile, 2D mode can be properly computed the vertical and east–west deformation due to the event of Lombok earthquake in 2018. The motion was validated with the result of Okada deformation, and it showed similar patterns of movement between InSAR decomposition and Okada modeling. However, it takes into account some limitations of these modes. Firstly, 3D mode only uses two InSAR look directions with an additional component under the slope aspect assumption. If a behaviour of landslide is a circular slide surface instead of a planar, then the expectation of motion straightly toward downhill is not acceptable. Secondly, 2D mode is still lack of one motion vector of north–south direction which is important to project on a horizontal movement. In an earthquake study, 3D displacement is critical to evaluate the source of earthquake and its behaviour based on the depth, strike, dip, length, width, rake, and slip.

PS DISP was created to help InSAR end-user interpreting the LOS perspective with a common geometric view. The output of 2D/3D vector displacement mainly corresponds to the quality of input LOS displacement of InSAR/PS processing. As noted in the introduction, each case study has different characteristics of displacement. If it only uses a combination ascending and descending interferogram, the third component should precisely reflect the actual geometry model based on its own geophysical characteristics. Some algorithms of 3D<sub>pseudo</sub> mode are needed to develop mathematical model of each geo-phenomenon, such as volcanic eruptions, landslide, glacier movement, *etc.* Another solution of 3D mode is to combine InSAR result to other ground measurements (*e.g.* GNSS measurement, ground-based radar interferometry, and extensometer) or optical imageries to especially retrieve the horizontal component.

#### APPENDIX

PS\_DISP (doi: 10.5281/zenodo.3757009) can be accessed on GitHub [https://github.com/dedetmix/PS\\_DISP](https://github.com/dedetmix/PS_DISP).

#### ACKNOWLEDGMENTS

The research was supported by Deutscher Akademischer Austauschdienst (DAAD) and funded by Directorate of Research and Community Service (DRPM), Institut Teknologi Sepuluh November. Sentinel-1 dataset was provided by Copernicus Open Access Hub, European Space Agency (ESA).

#### REFERENCES

- Arifianti, Y., Pamela, Agustin, F., and Muslim, D., 2020. Comparative Study among Bivariate Statistical Models in Landslide Susceptibility Map. *Indonesian Journal on Geoscience*, 7 (1), p.51-63. DOI: 10.17014/ijog.7.1.51-63
- Bechor, N.B.D. and Zebker, H.A., 2006. Measuring two-dimensional movements using a single InSAR pair. *Geophysical Research Letters*, 33 (16). L16311.
- Ding, X. and Huang, W., 2011. D-InSAR monitoring of crustal deformation in the eastern segment of the Altyn Tagh Fault. *International Journal of Remote Sensing*, 32 (7), p.1797-1806. DOI: 10.1080/01431160903490190.
- d Vigny, C., 2016. Three-dimensional displacement field of the 2015 Mw8.3 Illapel earthquake (Chile) from across- and along-track Sentinel-1 TOPS interferometry. *Geophysical Research Letters*, 43 (6), p.2552-2561. DOI: 10.1002 / 2016GL067954.
- Hanssen, R.F., 2001. Radar Interferometry: Data Interpretation and Error Analysis. *Remote Sensing and Digital Image Processing*, 2. Springer Netherlands.
- Hooper, A., 2008. A multi-temporal InSAR method incorporating both persistent scatterer and small baseline approaches. *Geophysical Research Letters*, 35 (16), pp. n/a-n/a. L16302.
- Hooper A., Bekaert D., Spaans K., and Arikan M., 2012. Recent advances in SAR interferometry time series analysis for measuring crustal deformation, *Tectonophysics*, 514-517, p.1-13. DOI: 10.1016/j.tecto.2011.10.013.
- Hu, J., Li, Z.W., Ding, X.L., Zhu, J.J., Zhang, L., and Sun, Q., 2014. Resolving three-dimensional surface displacements from InSAR measurements: A review. *Earth-Science Reviews*, 133, p.1 -17.
- Isya, N.H., Niemeier, W., and Gerke, 2019. M.3D Estimation of Slow Ground Motion Using InSAR and The Slope Aspect Assumption, A Case Study: The Puncak Pass Landslide, Indonesia, ISPRS Ann. Photogram. *Remote Sensing and Spatial Information Science*, IV-2/W5, p.623-630, DOI: 10.5194/isprs-annals-IV-2-W5-623-2019, 2019.
- Mohr, J.J., 1997. *Repeat Track SAR Interferometry. An investigation of its Utility for Studies of Glacier Dynamics. PhD thesis*. Technical University of Denmark, Copenhagen.

- Notti, D., Calo, F., Cigna, F., and Manuata, M., 2015. A User-Oriented Methodology for DInSAR Time Series Analysis and Interpretation: Landslides and Subsidence Case Studies. *Pure and Applied Geophysics*, 172 (11), p.3081-3105. ISSN: 1420-9136. DOI: 10.1007/s00024-015-1071-4.
- Okada, Y., 1985. Surface deformation due to shear and tensile faults in a half-space, *Bulletin of the Seismological Society of America*, 75, p.1435-1154.
- Okada, Y., 1992. Internal deformation due to shear and tensile faults in a half-space, *Bulletin of the Seismological Society of America*, 82, p.1018-1040.
- Provost, F. and Handwerker, A.L., 2018. Combining Sentinel-1 and Ground-based SAR to retrieve landslide 3D displacement: application to Pas de l'Ours landslide, France. URL: <https://agu.confex.com/agu/fm1/meetingapp.cgi/Paper/448147>.
- Ramdani, F., Setiani, P., and Setiawati, D., 2019. Analysis of sequence earthquake of Lombok Island, Indonesia. *Progress in Disaster Science*, 4, p.100046.
- Sadarviana, V., 2006. *Pemanfaatan Metode Geodetik untuk Mengestimasi Karakteristik Tipe dan Bidang Gelincir pada Zona Longsor; Wilayah Studi: Zona Longsor Ciloto-Puncak, Jawa Barat. PhD. thesis.* Institut Teknologi Bandung.
- Salman, R., Lindsey, E.O., Lythgoe, K.H., Bradley, K., Muzli, M., Yun, S.H., Chin, S.T., Tay, C.W.J., Costa, F., Wei, S., and Hill, E.M., 2020. Cascading partial rupture of the Flores thrust during the 2018 Lombok earthquake sequence, Indonesia. *Seismological Research Letters*, 91(4), p.2141-2151. DOI: 10.1785/0220190378.
- Sandwell, D., Rob, Xiaopeng, Xu, X., Wei, M., Wessel, P., 2016. *GMTSAR: An InSAR Processing System Based on Generic Mapping Tools (Second Edition)*. Scripps Institution of Oceanography, University of California, San Diego.
- Smith, W.H.F. and Wessel, P., 1990. Gridding with continuous curvature splines in tension. *Geophysics*, 55 (3), p.293-305. DOI: 10.1190/1.1442837.
- Vollrath, A., Zucca, F., Bekart, D., Bonvorte, A., Guglielmino, F., Hooper, A.J., and Stramondo, S., 2017. Decomposing DInSAR Time Series into 3-D in Combination with GPS in the Case of Low Strain Rates: An Application to the Hyblean Plateau, Sicily, Italy. *Remote Sensing*, 9 (1), 33pp. DOI: 10.3390/rs9010033.
- Wright, T.J., Parsons, B.E., and Lu, Z., 2004. Toward mapping surface deformation in three dimensions using InSAR. *Geophysical Research Letters*, 31 (1). DOI:10.1029/2003GL018827.